THE OPTICAL ABSORPTION CHANGES IN TWO-STEP INFINITE SPHERICAL QUANTUM DOT

Sevket Erol Okan[1,2], Hande Temel[2], Abdullah Bilekkaya[2,3], Figen Karaca Boz[1,2]

[1] Trakya University, Faculty of Science, Department of Physics, 22030 Edirne, Turkey
[2] Trakya University, Institute of Science, 22030 Edirne, Turkey
[3] Trakya University, Edirne Vocational College of Technical Sciences,22100 Edirne, Turkey

Abstract

Total absorption coefficients of $GaAs / Al_{x_1}Ga_{1-x_1}As / Al_{x_2}Ga_{1-x_2}As/AlAs$ infinite spherical quantum dots, which can be defined as a two-step potential profile, were calculated. Containing or not containing impurity atoms in the aforementioned structures were also taken into account. First, energies and wave functions were calculated with the effective mass approach using the Runge Kutta numerical method. For different layer (or step) thicknesses, 1s-1p, 1p-1d, and 1d-1f transition energies and total absorption coefficients were found. The results show that the presence of impurity atoms in the structure together with the structural geometry leads to interesting changes in the total absorption coefficients associated with the transitions of 1s-1p, 1p-1d, and 1d-1f.

Keywords: Spherical quantum dots, energies, optical absorption coefficient

INTRODUCTION

Semiconductor technology started with the invention of the transistor quite a few decades ago. Since then, too many successful research has been devoted to production of smaller and faster electronic and optoelectronic devices. Along these lines, nanotechnological research on low dimensional semiconducting structures cover an extensive field in the searches of new electronic devices [1]. One of these low-dimensional devices is quantum dots, also called zero-dimensional structure. The growth technology allows to obtain them in different geometric shapes such as rectangles, spheres, triangles, disks, etc. [2-6]. Therefore, the shape effect study on the optical and electronic properties of quantum dots has become a branch of research [2-6]. Same is also valid for the size effects [7,9]. In addition to these studies, many authors have considered the electronic properties of the ground and excited states in the view of their binding energies and radial probability distributions [8-18]. There are also different aspects with which the properties of quantum dots have been handled. These may be lined up as the hydrostatic pressure effects, the impurity and its location in the structure, magnetic and electric field effects, the linear and non-linear absorption, and the refractive index [19-24].

Jafari calculated the linear, non-linear total absorption coefficient of an impurity atom in an inhomogeneous spherical quantum dot, corresponding to 1s-2p, 2p-3d transitions. It has been observed that the optical properties are affected by the variation of inner radius and shell thickness of a two-layered quantum dot [8] . Tas and Sahin investigated the inter-level optical properties of spherical quantum dots and quantum wells with and without impurities depending on the core radius, well widths, and layer thicknesses [21]. Kavruk et al. have presented the optical transitions due to aluminum concentration x in the core and shell regions of $\mathbf{Al_xGa_{1-x}As/Al_{0.3}Ga_{0.7}As/Al_yGa_{1-y}As /Al_{0.3}Ga_{0.7}As}$ multilayered quantum dot [23].

In this study, the energy states and wave functions in $\mathbf{GaAs / Al_{x_1}Ga_{1-x_1}As / Al_{x_2}Ga_{1-x_2}As/AlAs}$ infinite spherical quantum dots are calculated considering both the presence and lack of an impurity atom.

520

Then, the total absorption coefficients of 1s-1p, 1p-1d, and 1d-1f with transition energies are reported using these aforementioned results.

THEORY

Let us consider two-step infinite spherical quantum dots as designed in Fig. 1. Taking the radius of the $GaAs$ sphere as R_1, the $Al_{x_1}Ga_{1-x_1}As$ layer thickness was defined as $R_2 = 2R_1 - R_1 = R_1$ and the $Al_{x_2}Ga_{1-x_2}As$ layer thickness as $R_3 = 3R_1 - 2R_1 = R_1$.
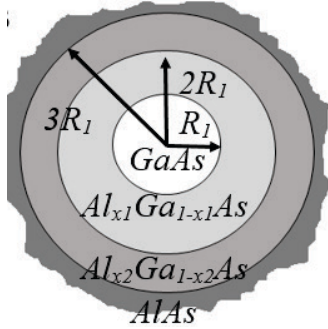

Fig 1. *The schematic representation of a two-step infinite spherical quantum dot.*

The three-dimensional time-independent Hamiltonian of an electron bound to an on-center impurity, in the units of effective Bohr radius $a^* = \varepsilon\hbar^2/me^2$ and Rydberg energy $R^* = me^4/2\hbar^2\varepsilon^2$ is given

$$H = -\nabla^2 + V(r) - Z\frac{2}{r} \qquad (1)$$

where $V(r)$ the potential energy of a two-step infinite spherical quantum dot;

$$V(r) = \begin{cases} 0, & 0 < r \leq R_1 \\ V_0, & R_1 < r \leq 2R_1 \\ 2V_0, & 2R_1 < r \leq 3R_1 \\ \infty, & r > 3R_1 \end{cases} \qquad (2)$$

is defined. In Eq.1, $Z = 0$ and $Z = 1$ correspond to the case without and with an impurity of structure, respectively. The eigenfunction of the Hamiltonian in Eq.1 is given by $\Psi_{nlm} = R_{nl}(r)Y_{lm}(\theta,\varphi)$, where $R_{nl}(r)$ is the radial wave function and $Y_{lm}(\theta,\varphi)$ is the spherical harmonics. Using these eigenfunctions, the following radial Schrödinger equation is obtained as

$$\frac{d^2R_{nl}(r)}{dr^2} + \frac{2}{r}\frac{dR_{nl}(r)}{dr} + \left[E_{nl} + Z\frac{2}{r} - V(r) - \frac{l(l+1)}{r^2}\right]R_{nl}(r) = 0 \qquad (3)$$

The energy levels E_{nl} and wavefunctions $R_{nl}(r)$ can be found from the solution of Eq.3 by using Runge-Kutta method [16].

By using the density matrix formalism, the optical properties may be defined as photo absorption occurring in initial state i (Ψ_i) to a final state f (Ψ_f). For the intersubband transitions, applying the Fermi golden rule, the total absorption coefficient is given by [20,24-27].

$$\alpha(\omega, I) = \alpha^1(\omega) + \alpha^3(\omega, I) \qquad (4)$$

The first and second terms on the right-hand side of Eq.4 are

$$\alpha^1(\omega) = \frac{\sigma}{\epsilon_0 n_r c}\frac{|M_{ij}|^2\hbar\omega\Gamma}{(E_{fi} - \hbar\omega)^2 + (\hbar\Gamma)^2}$$

and $\qquad (5)$

$$\alpha^3(\omega, I) = -\left(\frac{2I\sigma}{[\epsilon_0 n_r c]^2}\right)x\frac{|M_{ij}|^4\hbar\omega\Gamma}{[(E_{fi} - \hbar\omega)^2 + (\hbar\Gamma)^2]^2}$$

where n_r is the refractive index, Γ is the relaxation, I is the optical intensity of the incident wave. The transition energy

$$E_{fi} = E_f - E_i \qquad (6)$$

is the energy difference between the final and initial states. Assuming that the electromagnetic radiation is polarized throughout the z-axis, M_{if} is the dipole transition matrix element corresponding to i and f states that is given by

$$M_{if} = \left|e\int_0^{2\pi}\int_0^{\pi}\int_0^{\infty}\Psi_f r\cos\theta\Psi_i\, xr^2 dr\sin\theta d\theta d\varphi\right| \qquad (7)$$

RESULTS

We examine the electronic and optical properties in the presence and lack of the electron-bound impurity atom in the quantum dot shown in Fig. 1. The constants used in the calculations are $R^* = 5.25$meV, $a^* = 104$Å, $V_0 = 148meV$, electron density $\sigma=3\text{x}10^{22}\text{m}^{-3}$, $n_r=3.5$, $\Gamma=7.14\text{x}10^{12}\text{s}^{-1}$, I=400MW/m² [17,28].
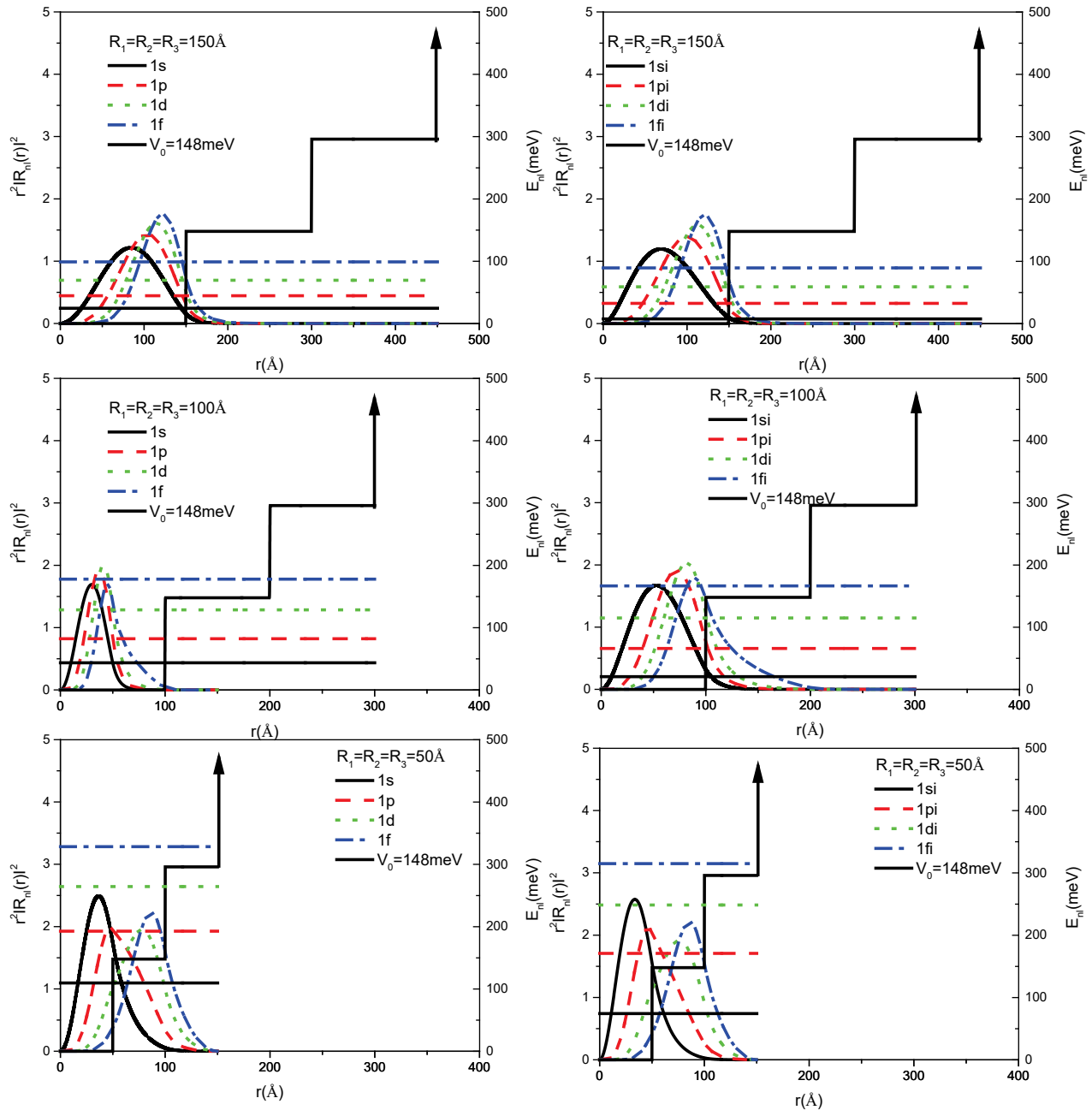
Fig. 2. *The energies and probability distributions of the states for different step thicknesses when the left column does not contain impurity atom in the structure, while the right column contains impurity atom in the structure.*

In the left column of Fig. 2, the energy states and probability densities of the quantum dot without impurity atoms were calculated for different step thicknesses. In the right column of the figure, the same calculations were performed for the same step thicknesses in the presence of impurity. It was observed that the energies decreased in both cases as the step thicknesses were increased. It has been observed that the probability densities are distributed over the entire structure for small

values of step thickness, while they were mostly localized to the GaAs region with increasing step thickness. It was determined that the energy states with impurity atom decreased when compared to the energy states in the absence of impurity atom.

To find the optical absorption coefficients, the transition energies defined in Eq.5 are shown as the functions of step thicknesses in Fig. 3. It was observed that the energy differences were large at small step thicknesses.

522

The difference between 1s-1p energies was the largest for step thickness 50 Å. As the step thickness increased, the mentioned energy difference decreased. It was observed that the differences between the transition energies at the critical step thicknesses were close to each other. In a structure without impurity atom, the difference between 1s-1p and 1p-1d energies around 70 Å is almost the same. The 1d-1f energy difference remained constant over the 70 Å to 110 Å step thickness range. It was observed that the 1d-1f energy differences were larger than the other energy differences for thicknesses above 110 Å. Similar behavior was observed in the quantum dot containing impurity atom. However, it was determined that the energy differences were close to each other for large step thicknesses.
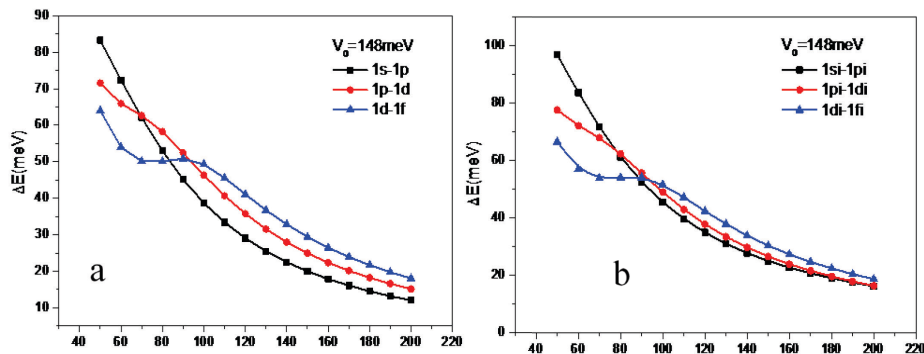

Fig. 3. *Transition energies depending on step thicknesses a) in the absence of an impurity atom and b) in the presence of an impurity atom.*

In Fig. 4, the change in the total optical absorption coefficient associated with 1s-1p, 1p-1d, and 1d-1f transitions in the absence of impurity atom is plotted as a function of incident photon energy, for different step thicknesses. The photon energy values at which the absorption coefficient is maximum show the same behavior in all three transitions with the increase in step thickness. If the step thickness increased from 50 Å to 100 Å, the absorption coefficients reach their maximum values at smaller photon energies. The reason for this behavior can be explained by the probability density shown on the left side of Fig.2 in the narrow structure and the energy differences in Fig.3. Note that the wavefunction probability density spans the entire quantum dot at small step thicknesses. The wave functions of all states with step thicknesses of 100 Å are in the GaAs region. At 150 Å step thickness, the probability densities slightly extend beyond the GaAs region. When we look at the energy differences in Fig. 3a, we see that the 1s-1p energy difference for 50 Å is larger
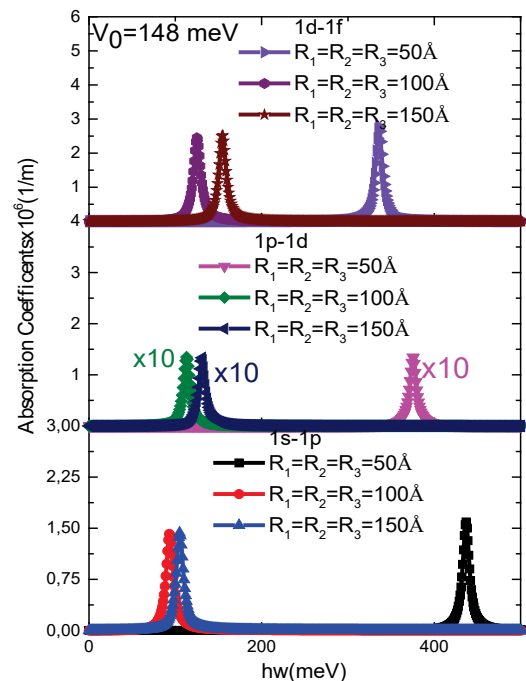

Fig. 4. *Total absorption coefficients as a function of incident photon energy for the 1s-1p, 1p-1d, and 1d-1f transition without impurity.*

than the 1p-1d and d-1f energy differences. The energy differences for 100 Å appear to be the same for all cases. We think that the probability density of the wavefunctions may be effective for this step's thickness. When we look at the energy differences for the 150 Å step thickness, it is seen that the 1d-1f, 1p-1d, and 1s-1p transitions are, ordered from the largest to the smallest. The photon energies giving the maximum absorption coefficient show the same trend. Concerning graph shows that the step thickness affects the total optical absorption coefficients in two-stepped infinite spherical quantum dots.
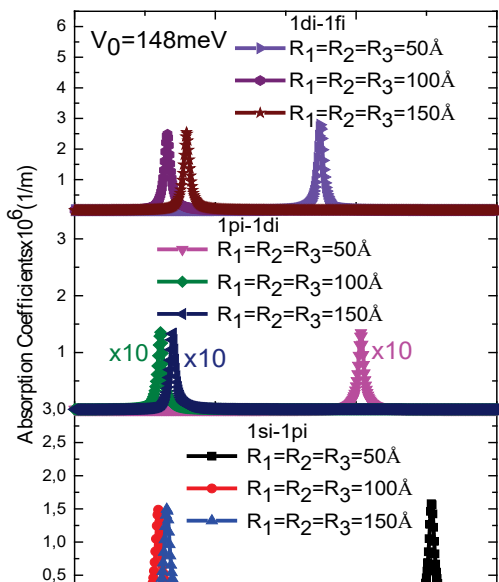

Fig. 5. Total absorption coefficients as a function of incident photon energy for the 1s-1p, 1p-1d, and 1d-1f transition with impurity.

To examine the effect of impurity atom in the structure, the variation total absorption coefficients of 1s-1p, 1p-1d, and 1d-1f transitions depending on the incident photon energy are plotted in Fig. 5 by considering different step thicknesses. The behavior of the resulting functions is similar to their counterparts in the impurity-free state given in Fig. 4. In addition, in the presence of the impurity atom, the probability density does not change much compared to the absence of the

impurity atom. When the same comparison is made for the photon energy values that make the absorption coefficients the largest, differences are observed between the impurity-present and impurity-absent states due to the difference in energy changes. For 50 Å step thickness, the transition energies between energy states shift to small photon energies, while 100 Å step thickness it shows the maximum absorption coefficient at almost the same photon energy value. Because the energy differences between the transitions are almost equal to each other. It was observed that the transition energies between energy states shifted toward larger values for the 150 Å step thickness. This is because the probability distribution of the impurity electron is localized to the GaAs region.

CONCLUSION

As summary, some interesting behaviors were observed when the energies and wave functions for the states with and without foreign atoms in $GaAs \, / \, Al_{x_1}Ga_{1-x_1}As \, / \, Al_{x_2}Ga_{1-x_2}As \, / \, AlAs$ infinite spherical quantum dots were examined depending on the step thickness. According to these results, the total absorption coefficients were calculated depending on the photon energy. It was observed that both presence and absence of impurities and step thickness were effective on the total absorption coefficients.

REFERENCES

[1] Ünlü, H., & Horing, N. J. Low Dimensional Semiconductor Structures Characterization, Modeling and Applications. Springer 2013.

[2] Harrison, P. Quantum Wells, Wires and Dots (3. b.). England: WILEY 2009.

[3] Khordad, R., & Bahramiyan, H. Impurity position effect on optical properties of various quantum dots. Physica E (2015); (66): 107-115.

[4] Barseghyan, M. G., Restrepo, R. L., Mora-Ramos, M. E., & Kirakosyan, A. A. Donor impurity-related linear and nonlinear intraband optical absorption coefficients in the quantum ring: effect of applied electric field and hydrostatic pressure. Nanoscale Research Letters. (2012); 7(1):538.

[5] Restrepo, R. L., Barseghyan, M. G., Mora-Ramos, M. E., & Duque, C. A. Effects of hydrostatic pressure on the nonlinear optical properties of a donor impurity in a GaAs quantum ring. Physica E (2013); (51): 48-54.

524

[6] Rani, P., Dalal, R., & Srivastava, S. Study of electronic and optical properties of quantum dots. Applied Nanoscience, (2022); 12; 2127–2138.

[7] Ledentsov, N. N., Ustinov, V. M., Shchukin, V. A., Kop'ev, P. S., & Alferov, Z. I. Quantum dot heterostructures: fabrication, properties, lasers. Semiconductors, (1998); 32(4): 385–410.

[8] Jafari, A. R. Optical properties of hydrogenic impurity in an inhomogeneous infinite spherical quantum dot. Physica B, (2015); 456: 72-77.

[9] Yılmazer, F., Yakar, Y., Çakır , B., & Özmen, A.. Küresel Kuantum Nokta Yapının Elektronik Yapısı ve Bağlanma Enerjisi. DergiPark (2017); (1): 41-52.

[10] ZHU, J., XIONG, J., & GU, B. Confined Electron and the Hydrogenic Donor States in a Spherical Quantum Dot of GaAs-Ga1-xAlxAs. Physical Review B, (1990); 41(9): 6001-6007.

[11] Bose, C., & Sarkar, C. K. Perturbation Calculation Of Donor States in a Spherical Quantum Dot. Pergamon (1998); (42): 1661-1663.

[12] Aktas, S., & Karaca Boz, F. The Binding Energy of hydrogenic impurity in multilayered spherical quantum dot. Physica E: Low-dimensional Systems and Nanostructures (2008); (40): 753-758.

[13] Çakır, B., Sezer, M. Ö., Yakar, Y., Özmen, A., & Yüksel, H. Hidrojen Tipi Kuantum Nokta Yapının Taban Durumunun Kuantum Genetik Algoritma Yöntemiyle İncelenmesi. Selçuk Üniversitesi Fen Fakültesi Fen Dergisi (2009); 33: 45-49.

[14] Sadeghi, E. Impurity binding energy of excited states in spherical quantum dot. Physica E (2009); 41: 1319-1322.

[15] De Souza, G. V., & Bruno-Alfonso, A. Finite-difference calculation of donor energy levels in a spherical quantum dot subject to a magnetic field. Physica E (2015); 66:, 128-132.

[16] Karaca Boz, F., Nisancı, B., Aktas, S., & Okan, S. O. Energy levels of GaAs/AlxGa1-xAs/AlAs spherical quantum dot with an impurity. Applied Surface Science (2016);. 387: 76-81.

[17] Al, E. B., Kasapoglu, E., Sakiroglu, S., Sari, H., Sökmen, I., & Duque, C. A. Binding energies and optical absorption of donor impurities in spherical quantum dot under applied magnetic field. Physica E: Low-dimensional Systems and Nanostructures (2020); 119:.1-8.

[18] Rabanian, A., Neghabi, M., Zadsar, M., & Jafari, M. Theoretical studies of energy states of CdSe/ZnS/CdSe and ZnS/CdSe/ZnS quantum dots with an impurity. Materials Science & Engineering B (2021); 274;1-7.

[19] Özmen, A., Yakar, Y., Çakır, B., & Atav, Ü. Computation of the oscillator strength and absorption coefficients for the intersubband transitions of the spherical quantum dot. Optics Communications (2009); 282: 3999-4004.

[20] Çakır, B., Yakar, Y., Özmen, A., & Sezer, M. Ö. Linear and nonlinear optical absorption coefficients and binding energy of a spherical quantum dot. Superlattices and Microstructures (2010); 47: 556–566.

[21] Taş, H., & Şahin, M .The inter-sublevel optical properties of a spherical quantum dot- quantum well with and without a donor impurity. Journal of Applied Physics, (2012); 112(5): 053717

[22] Kirak, M., Altinok, Y., & Yilmaz, S. The effects of the hydrostatic pressure and temperature on binding energy and optical properties of a donor impurity in a spherical quantum dot under external electric field. Journal of Luminescence (2013); 136: 415-421.

[23] Kavruk, A. E., Sahin, M., & Atav, U. A detailed investigation of electronic and intersubband optical properties of AlxGa1−xAs/Al0.3Ga0.7As/AlyGa1−yAs/Al0.3Ga0.7As multi-shell quantum dots. Journal of Physics D Applied Physics (2014); 47(29):295302.

[24] Liu, W. H., Qu, Y., & Ban, S. L. Intersubband optical absorption between multi energy levels of electrons in InGaN/GaN spherical core-shell quantum dots. Superlattices and Microstructures (2017); 102: 373-381.

[25] Bekar, B., Boz, F. K., Aktas, S., & Okan, S. E. The Effect on the Optical Absorption Coefficients due to the Positions in the Plane of Square GaAs / Al(GaAs) Quantum Well Wire under the Laser Field. ACTA PHYSICA POLONICA A (2019); 136(6):882-888

[26] Al, E. B. Effect of the magnetic field, size and donor position on the absorption coefficients related to a donor within the core/shell/shell quantum dot. Optical and Quantum Electronics, (2021); 53(676):1-15.

[27] En-nadir, R., El Ghazi, H., Belaid, W., Abboudi, H., Jabouti, F., Jorio, A., & Zokani, I. The Confinement Profile Effect on the Optical Properties in Different Inverseshaped Single InGaN/GaN Quantum Wells. Iraqi Journal of Physics, (2022). 20(1): 1-13.

[28] Kavruk A. E., Sahin M., Atav Ü. A detailed investigation of electronic and intersubband optical properties of AlxGa1-xAs/Al0.Ga0.7As/AlyGa1-yAs/Al0.3Ga0.7As multi-shell quantum dots. J. Phys. D: Appl. Phys. (2014); 47(295302):1-8.

525